

LA-8647

2

Jet Initiation of Explosives

DO NOT CIRCULATE

PERMANENT RETENTION

REQUIRED BY CONTRACT

University of California

LOS ALAMOS NATIONAL LABORATORY



3 9338 00307 0751



LOS ALAMOS SCIENTIFIC LABORATORY

Post Office Box 1663 Los Alamos, New Mexico 87545

Edited by Sharon L. Crane

Photocomposition by Alice Creek

DISCLAIMER

This report was prepared as an account of work sponsored by an agency of the United States Government. Neither the United States Government nor any agency thereof, nor any of their employees, makes any warranty, express or implied, or assumes any legal liability or responsibility for the accuracy, completeness, or usefulness of any information, apparatus, product, or process disclosed, or represents that its use would not infringe privately owned rights. Reference herein to any specific commercial product, process, or service by trade name, trademark, manufacturer, or otherwise, does not necessarily constitute or imply its endorsement, recommendation, or favoring by the United States Government or any agency thereof. The views and opinions of authors expressed herein do not necessarily state or reflect those of the United States Government or any agency thereof.

**UNITED STATES
DEPARTMENT OF ENERGY
CONTRACT W-7405-ENG. 36**

LA-8647

UC-45

Issued: February 1981

Jet Initiation of Explosives

Charles L. Mader
George H. Pimbley



JET INITIATION OF EXPLOSIVES

by

Charles L. Mader and George H. Pimbley

ABSTRACT

The initiation of propagating detonation in PBX 9502 and PBX 9404 by jets of copper, aluminum, and water is numerically modeled using the two-dimensional Eulerian hydrodynamic code 2DE with the shock initiation of heterogeneous explosive burn model called Forest Fire.

The Held experimental critical condition for propagating detonation is the jet velocity squared times the jet diameter. In PBX 9502, the jets initiate an overdriven detonation smaller than the critical diameter, which either fails or enlarges to greater than the critical diameter while the overdriven detonation decays to the C-J state.

In PBX 9404 the jet initiates a detonation that propagates only if it is maintained by the jet for an interval sufficient to establish a stable curved detonation front.

I. INTRODUCTION

The process of shock initiation of heterogeneous explosives has been modeled¹ for many shock sensitivity tests using the Forest Fire rate model and the reactive hydrodynamic codes SIN, 2DL, and 2DE. The basic mechanism of heterogeneous explosive shock initiation is shock interaction at density discontinuities producing local hot spots that decompose and add their energy to the flow. Forest Fire models the gross features of this flow. Calculations have modeled the effect of drivers or projectiles producing effectively one-dimensional shock waves in explosives with pressure less than the C-J detonation pressure and with varied durations.¹ Sympathetic detonation, the detonation of nearby explosive objects by the blast from a primary explosion, has been numerically modeled using the Eulerian reactive hydrodynamic code 2DE with Forest Fire burn rates.² The gap sensitivity test, where the shock from a standard donor explosive is transmitted to a test explosive through an inert barrier (gap), has been numerically modeled for both Los Alamos National Laboratory and Naval

Ordnance Laboratory tests.³ The minimum priming charge test, where the least mass of booster explosive is determined that will induce propagating detonation in a test charge, has been modeled by Forest⁴ using the SIN code with Forest Fire. The PBX 9501 initiation by steel cylinders and spheres has been studied by Cort and Fu,⁵ using the 2DE code with Forest Fire. These shock initiation experiments depend upon the magnitude and duration of the initiating shock wave being sufficient for buildup to detonation. When a detonation occurs, it propagates throughout the explosive if the charge diameters are larger than the failure diameter.

The failure diameter is the smallest explosive charge diameter that can maintain a propagating C-J detonation. The failure diameter is smaller if the charge is confined. The failure diameter of unconfined PBX 9502 is 0.9 cm and of PBX 9404 is 0.12 cm. This large difference is caused by the shock initiation properties of the explosives and can be modeled using the Forest Fire heterogeneous shock initiation burn model as described in Ref. 1. Corner turning in a propagating detonation is also a function of the shock initiation properties, as

shown in Ref. 1 for detonations propagating around air and metal corners and in Ref. 6 for detonations propagating from spherical initiators.

Heterogeneous explosive desensitization with a shock whose pressure is too low and too short in duration to cause propagating detonation can cause failure of a propagating detonation in unshocked explosive to continue propagating when the detonation front arrives at the previously shocked explosive. This process has been numerically modeled in Ref. 7. The Forest Fire burn rate is determined primarily by the initial shock pressure passing through the explosive.

We conclude that the heterogeneous shock initiation process dominates not only the buildup to detonation, but also how the detonation propagates when side or rear rarefactions are affecting the flow.

The type of sympathetic detonation that we investigate in this report is the explosive initiation by a nearby shaped charge with a metal cone that forms small-diameter, high-velocity projectiles.

The process was investigated first by Held.⁸ He used a shaped charge to drive a 1.5-mm-thick, 60° copper cone. The resulting copper jet was shot into steel plates of varying thickness to obtain different exit jet velocities. The jet sizes and velocities were measured using velocity screens and x-ray flash photography. The jets were permitted to interact with an explosive, and the critical velocity was determined for initiation of propagating detonation by various diameter jets.

Held observed that his data could be correlated by assuming that the critical jet value for explosive initiation was the jet velocity squared (V^2) times the jet diameter (d). If the velocity is in millimeters per microsecond and the jet diameter is in millimeters, he reported that the critical V^2d was about 5.8 for copper jets initiating 60/40 RDX/TNT at 1.70 g/cm³.

Similar experiments have been performed by A. W. Campbell at the Los Alamos National Laboratory with copper jets initiating PBX 9404 (94/3/3 HMX/nitrocellulose/tris-β-chloroethyl phosphate at 1.844 g/cm³) and PBX 9502 (95/5 TATB/Kel-F at 1.894 g/cm³), and his data is summarized in Table I. Critical V^2d values are 127 ± 5 mm³/μs² for PBX 9502, 16 ± 2 mm³/μs² for PBX 9404, 37 mm³/μs² for 75/25 Cyclotol, and 29 mm³/μs² for Composition B-3.

If the pressure-particle velocity is matched, as shown in Fig. 1 for copper at 5.0 mm/μs shocking inert PBX 9502, the pressure match is 680 kbar; at 6.0 mm/μs the pressure match is 920 kbar. Since the C-J pressure of PBX 9502 is 285 kbar, the copper jet must initiate a

TABLE I
CAMPBELL EXPERIMENTAL DATA

Copper Jet Tip Velocity (mm/μs)	Jet Diameter (mm)	Result	V^2d (mm ³ /μs ²)
PBX 9502			
		Critical	127 ± 5
4.59	5.88	Detonation	124
4.47	5.96	Fail	119
4.65	5.84	Detonation	126
4.52	5.92	Fail	121
4.94	4.15	Fail	101
5.56	3.95	Fail	122
5.55	3.95	Fail	122
5.81	3.80	Detonation	128
5.93	3.85	Detonation	135
PBX 9404			
		Critical	16 ± 2
2.87	2.04	Detonation	16.8
2.51	2.25	Fail	14.2
2.76	2.11	Fail	16.0
3.07	1.95	Detonation	18.4
3.07	1.95	Detonation	18.4

strongly overdriven detonation. However, the jet diameter (~4 mm) is less than half the failure diameter (9.0 mm) of unconfined PBX 9502.

Also shown in Fig. 1, the pressure match is 340 kbar for PBX 9404 shocked initially by copper at 3.0 mm/μs and is 250 kbar at 2.5 mm/μs. The run distance for PBX 9404 at 250 kbar is about 0.5 mm so detonation would occur very quickly. The jet diameter (~2 mm) is larger than the unconfined PBX 9404 failure diameter (1.2 mm).

We shall examine the dominant mechanisms of jet initiation of PBX 9404 and PBX 9502 using the Forest Fire burn rate and the 2DE code.

II. NUMERICAL MODELING

The two-dimensional reactive Eulerian hydrodynamic code 2DE¹ was used to describe the reactive fluid dynamics. The Forest Fire description of heterogeneous shock initiation was used to describe the explosive burn. The HOM equation of state and Forest Fire rate constants for PBX 9502 and PBX 9404 were identical to

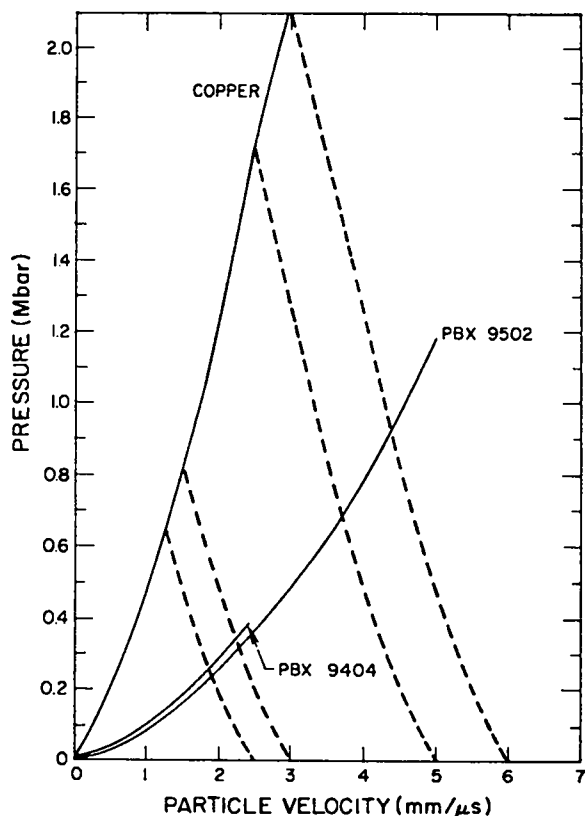


Fig. 1.

The pressure-particle velocity Hugoniots for copper, PBX 9502, and PBX 9404 with the reflected shock states for copper with initial free-surface velocities of 6.0, 5.0, 3.0, and 2.5 mm/μs.

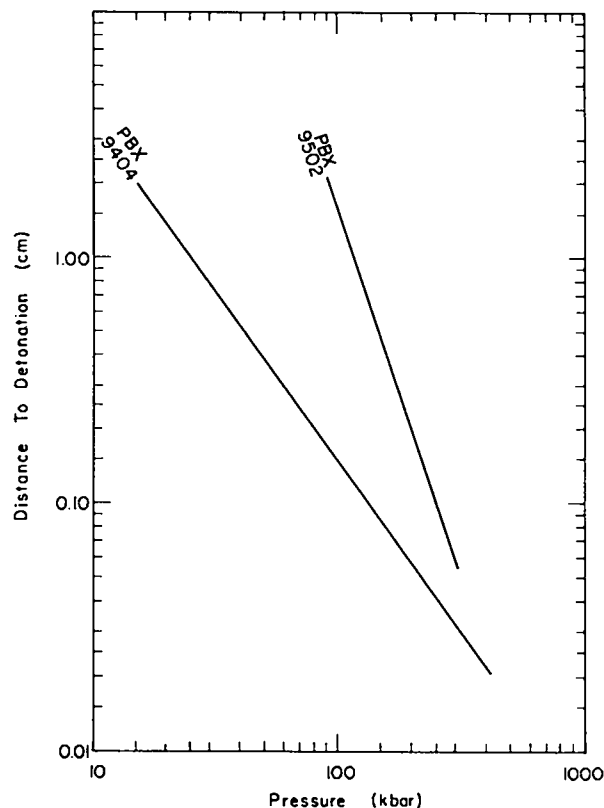


Fig. 2.

The run to detonation distance as a function of the shock pressure.

those described in Ref. 1. The Pop plots are shown in Fig. 2, and the Forest Fire rates are shown in Fig. 3.

The jet was described as a cylinder of radius 10 or 20 cells and 40 cells long with the appropriate initial velocity. The cell size was 0.02, 0.01, or 0.005 cm, depending upon the jet radius. The BPCJ term in Forest Fire was set at 1.5 to permit overdriven detonations and the rate was limited to e^{20} . The viscosity coefficient used for PBX 9502 was 0.25 and for PBX 9404 was 0.75. Sufficient viscosity to result in a resolved burn was necessary just as in the detonation failure calculations discussed in Refs. 1, 6, and 7.

An uncertainty in the calculations is the approximation of the jet as a cylinder of uniform velocity colliding end-on with the explosive. Although the jet is actually many small metal pieces, our calculations indicate that the critical conditions are determined by the first piece of about the same length as its radius. Side rarefactions dominate the flow after the reflected shock wave travels one diameter length back into the jet.

One also needs to consider the proper initial conditions for the jet. Since it was formed by being shocked and then rarefied, it will have a residual temperature greater than ambient and density less than the initial density of the jet material.

Estimates of the copper residual state can be made by assuming the material is at the same state as if it had achieved its final velocity by a single shock and then had rarefied to one atmosphere. The residual temperature of copper initially shocked to 830 kbar and then rarefied to a free-surface velocity of 3.0 mm/μs is 768 K; the residual density is 8.688 g/cm³, comparable with the initial density of 8.903. Calculations were performed with copper initial conditions of 8.903 g/cm³ and 300 K and of 8.688 g/cm³ and 768 K. Since the changed equation of state results in only slightly changed explosive shock pressure, the calculated results were insensitive to the copper jet initial conditions.

Another uncertainty is how accurately the Forest Fire burn rate can be extrapolated to overdriven detonations.

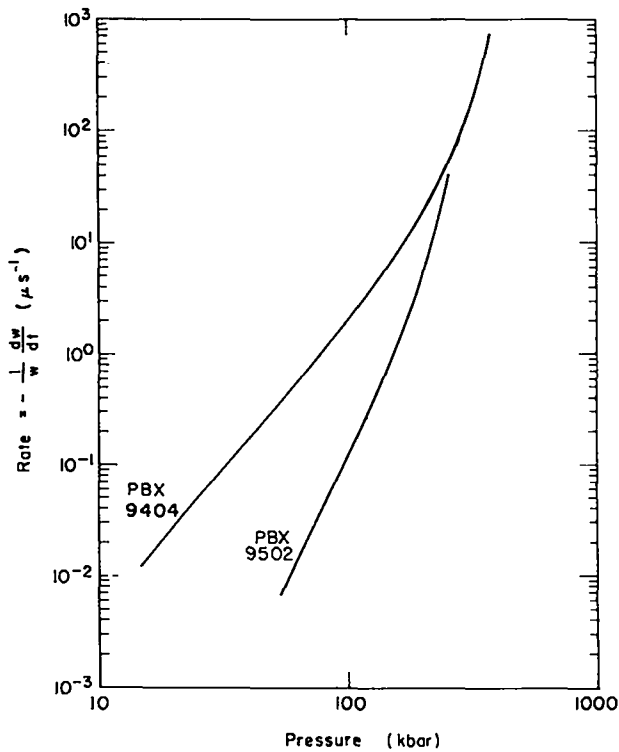


Fig. 3.

The Forest Fire decomposition rates as a function of shock pressure.

Since the overdrive decays rapidly and the side rarefactions quickly reduce the failure region pressure into the pressure range where the Pop plot was determined, the accuracy of the extrapolated burn rates is not important to the determination of the critical conditions for establishing propagating detonations.

The calculated PBX 9502 results are presented in Table II. The effects of jet composition, diameter, and velocity were examined. The calculated profiles for a 4-mm-diam copper jet with a 7.0-mm/ μ s initial velocity are shown in Fig. 4 and a 5.0-mm/ μ s velocity in Fig. 5.

The copper jet initiates an overdriven detonation smaller than the critical diameter, which enlarges to greater than the critical diameter of self-confined PBX 9502 when shocked by a 7.0-mm/ μ s copper jet. When the PBX 9502 is shocked by a 5.0-mm/ μ s copper jet, the detonation is decayed by side and rear rarefactions before it enlarges to the critical diameter.

As shown in Table II, the numerical results bound the Campbell experimental critical V^2d of 127 for copper jets. The shock pressure sent into the explosive depends upon the jet material, so the aluminum jet must have a greater velocity or diameter than the copper jet to furnish

an equivalent impulse to the PBX 9502. One then expects that the critical V^2d is larger for aluminum than for copper and larger still for a water jet. These conclusions are confirmed by the calculations with the predicted V^2d for aluminum being 325 ± 75 and for water about 800.

The calculated PBX 9404 results are presented in Table III. The effects of jet composition, diameter, and velocity were examined. The calculated profiles for a 2-mm-diam copper jet with a 3.0-mm/ μ s initial velocity are shown in Fig. 6, and a velocity of 2.0 mm/ μ s in Fig. 7. The copper jet initiates detonation, which propagates only if it is maintained by the jet long enough to establish a stable curved detonation front.

As shown in Table III, the numerical results bound the Campbell experimental critical V^2d of 16 for copper jets initiating propagating detonation in PBX 9404. The calculated results suggest a lower value for V^2d but one as accurate as the data and the approximations of the calculations. Again, the calculated, critical V^2d is larger for aluminum jets (70 ± 20) than copper jets and larger still for water jets (150 ± 50).

TABLE II

PBX 9502 CALCULATIONS

Jet Material	Jet Diameter (mm)	Jet Velocity (mm/ μ s)	Result	V^2d
Copper	4.0	4.0	Failed	64
Copper	4.0	5.0	Failed	100
Copper	4.0	6.0	Marginal	144
Copper	4.0	7.0	Propagated	196
Copper	8.0	4.0	Marginal	128
Copper	8.0	5.0	Propagated	200
Aluminum	4.0	7.0	Failed	196
Aluminum	4.0	8.0	Failed	256
Aluminum	4.0	10.0	Propagated	400
Aluminum	8.0	7.0	Propagated	392
Water	4.0	6.0	Failed	144
Water	4.0	10.0	Failed	400
Water	4.0	14.0	Marginal	784

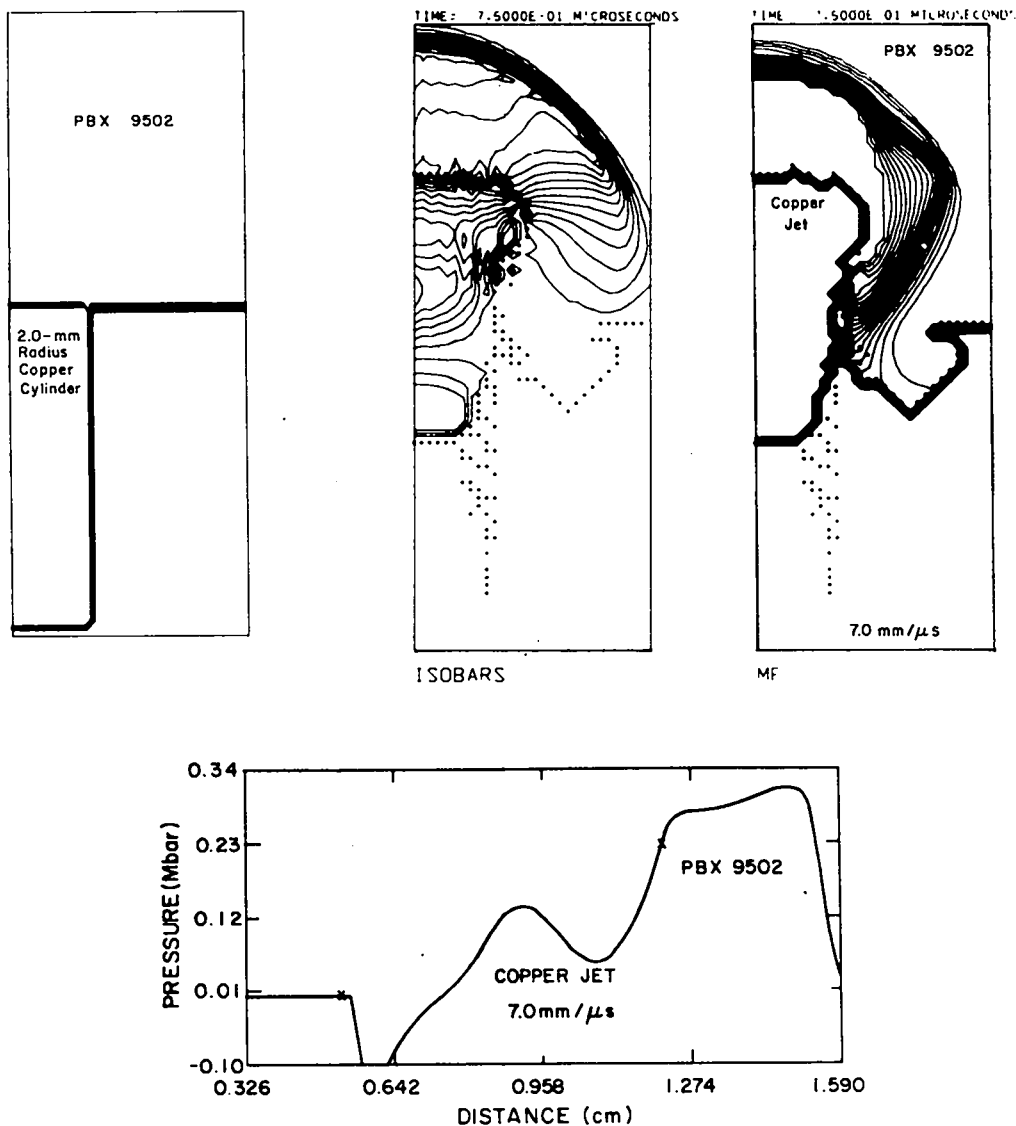


Fig. 4. The initial profile and the pressure and mass fraction profiles for a 4-mm-diam copper jet of 7.0 mm/ μ s shocking PBX 9502 at 0.75 μ s. The isobar contour interval is 20 kbar and the mass fraction contour is 0.05. The pressure profile along the axis is also shown.

III. CONCLUSIONS

The initiation of propagating detonation in PBX 9502 and PBX 9404 by jets of copper, aluminum, and water has been numerically modeled using the two-dimensional Eulerian hydrodynamic code 2DE with Forest Fire.

Shock initiation by jets near the critical V^2d contrasts with other shock initiation studies. In the latter, if detonation occurred, it was because the initiating shock

wave was of sufficient strength and duration to build up to detonation. The propagating detonation was assured by the large geometry. In near-critical jet initiation, however, a *prompt* detonation of the explosive results, which builds to a propagating detonation only if the shock wave produced by the jet is of sufficient magnitude and duration. Therefore, jets may produce significant amounts of energy from an explosive even below the critical value of V^2d required for propagating detonation.

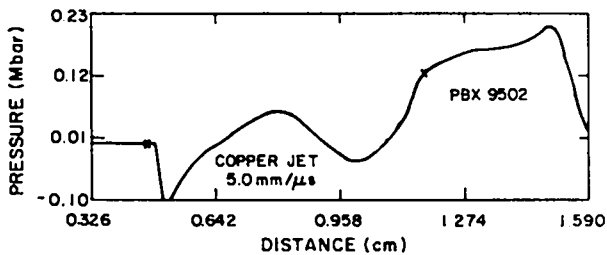
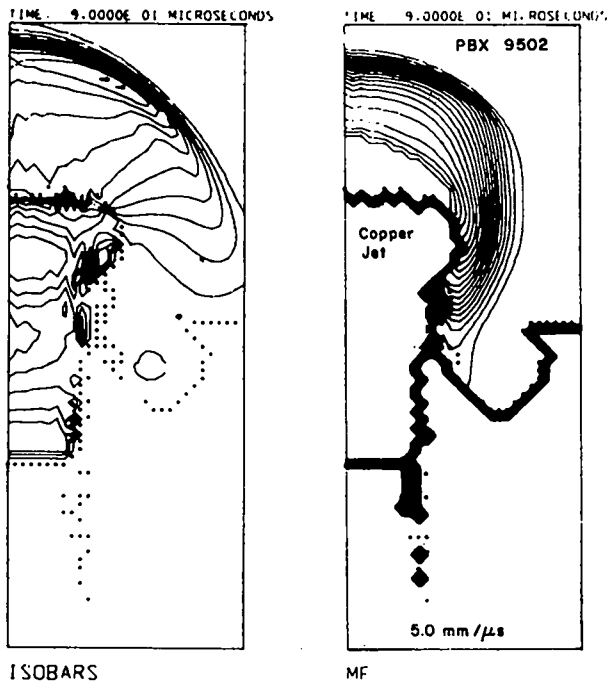


Fig. 5.

The pressure and mass fraction profiles for a 4-mm-diam copper jet of 5.0 mm/μs shocking PBX 9502 at 0.90 μs. The isobar contour interval is 20 kbar and the mass fraction contour is 0.05. The pressure profile along the axis is also shown.

TABLE III
PBX 9404 CALCULATIONS

Jet Material	Jet Diameter (mm)	Jet Velocity (mm/μs)	Result	V ² d
Copper	2.0	2.0	Failed	8
Copper	2.0	2.5	Marginal	12.5
Copper	2.0	3.0	Propagated	18
Copper	4.0	2.0	Propagated	16
Copper	4.0	2.5	Propagated	25
Copper	1.5	3.0	Marginal	13.5
Aluminum	2.0	3.0	Failed	18
Aluminum	2.0	6.0	Propagated	72
Aluminum	4.0	3.0	Failed	36
Aluminum	4.0	4.0	Marginal	64
Aluminum	4.0	6.0	Propagated	144
Water	4.0	3.0	Failed	36
Water	4.0	6.0	Marginal	144
Water	4.0	7.0	Propagated	196

IV. ACKNOWLEDGMENTS

The authors gratefully acknowledge the contributions, encouragement, and data of Arthur W. Campbell, the support of Larry Hantel, and the contributions of Charles Forest, Allen Bowman, and James Kershner. We also acknowledge the helpful discussions with Dr. M. Heid of MBB-Schrobenhausen.

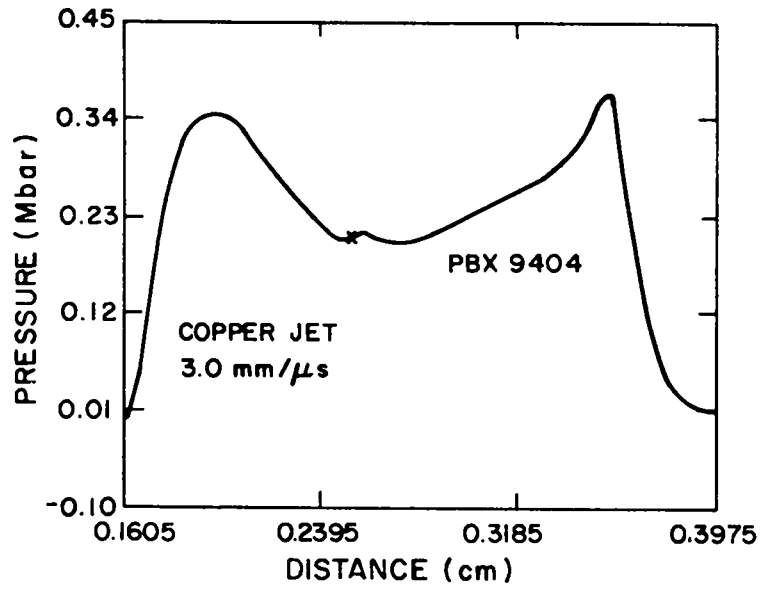
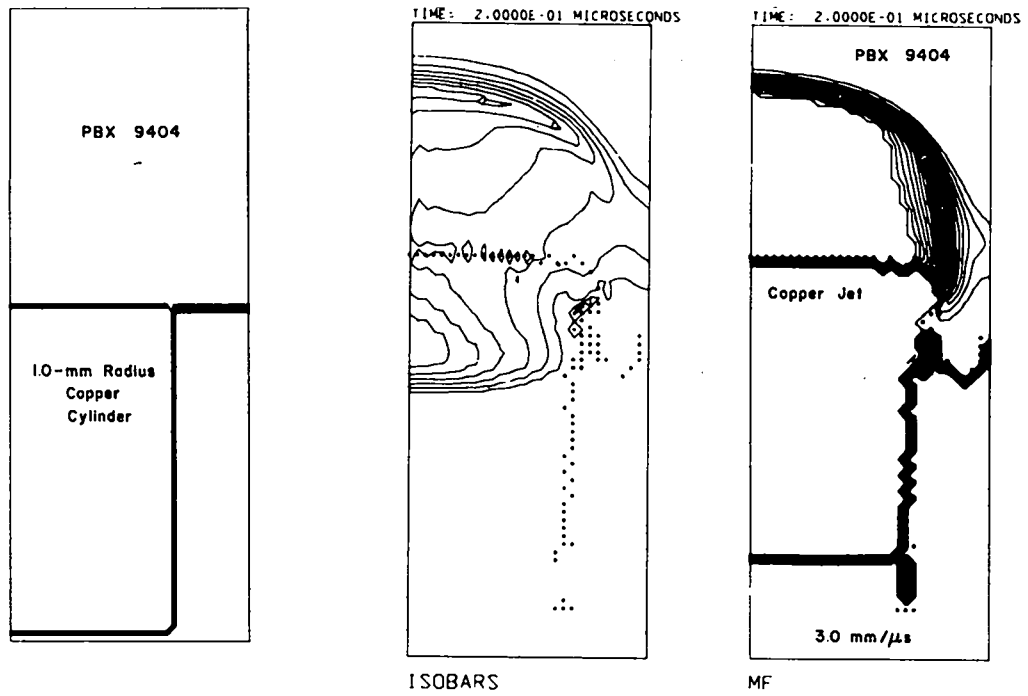


Fig. 6.
The initial profile and pressure and mass fraction profiles for a 2-mm-diam copper jet of 3.0 mm/μs shocking PBX 9404 at 0.20 μs. The isobar contour intervals is 50 kbar and the mass fraction contour is 0.05. The pressure profile along the axis is also shown.

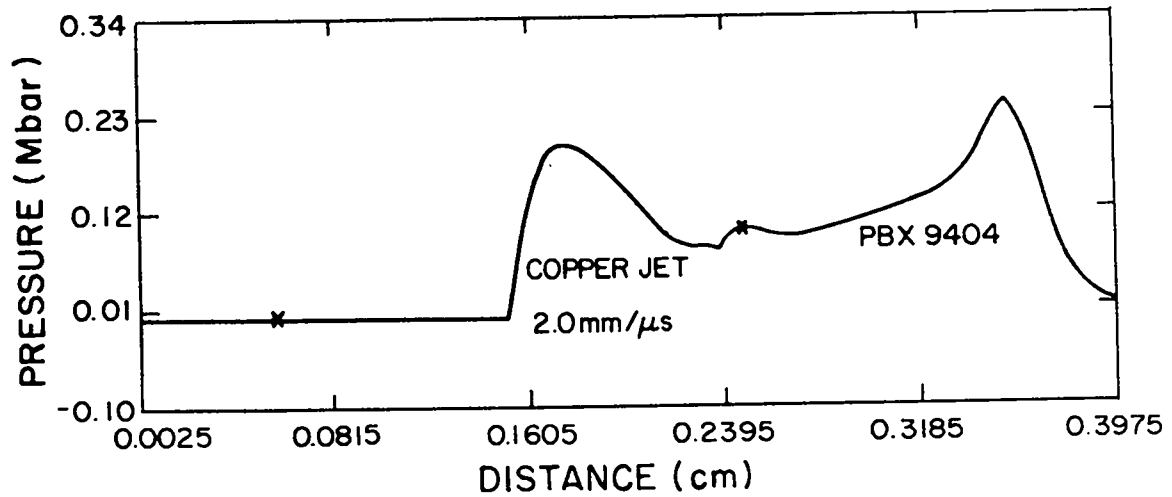
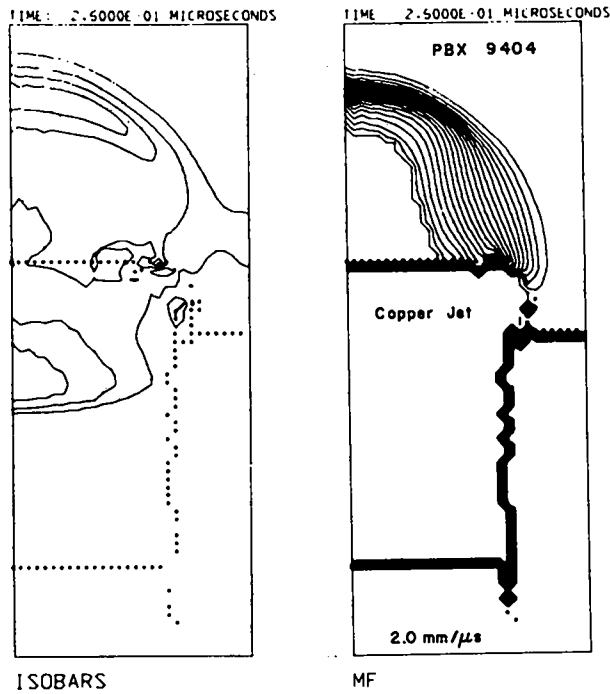


Fig. 7.
 The pressure and mass fraction profiles for a 2-mm-diam copper jet of 2.0 mm/μs shocking PBX 9404 at 0.25 μs. The isobar contour interval is 50 kbar and the mass fraction contour is 0.05. The pressure profile along the axis is also shown.

REFERENCES

1. Charles L. Mader, *Numerical Modeling of Detonations* (University of California Press, Berkeley, 1979).
2. Allen L. Bowman, James D. Kershner, and Charles L. Mader, "Numerical Modeling of Sympathetic Detonation," Los Alamos National Laboratory report LA-7989 (1979).
3. Allen L. Bowman, James D. Kershner, and Charles L. Mader, "A Numerical Model of Gap Test," Los Alamos National Laboratory report LA-8408 (1980).
4. Charles A. Forest, "Numerical Modeling of the Minimum Priming Charge Test," Los Alamos National Laboratory report LA-8075 (1980).
5. G. E. Cort and J. H. M. Fu, "Numerical Calculation of Shock-Induced Initiation of Detonations," JANNAF 1980 Propulsion Systems Hazards Meetings, Monterey, California, October 27-31, 1980.
6. Charles L. Mader, "Numerical Modeling of Insensitive High Explosive Initiators," Los Alamos National Laboratory report LA-8437-MS (1980).
7. Charles L. Mader and Richard Dick, "Explosive Desensitization by Preshocking," in *Combustion and Detonation Processes*, Internationale Jahrestagung, June 27-29, 1979 (Karlsruhe, Bundesrepublik Deutschland, 1979), pp. 569-579.
8. M. Held, "Initiating of Explosives, a Multiple Problem of the Physics of Detonation," *Explosivstoffe* 5, 98-113 (1968).

Printed in the United States of America
 Available from
 National Technical Information Service
 US Department of Commerce
 5285 Port Royal Road
 Springfield, VA 22161
 Microfiche \$3.50 (A01)

Page Range	Domestic Price	NTIS Price Code	Page Range	Domestic Price	NTIS Price Code	Page Range	Domestic Price	NTIS Price Code	Page Range	Domestic Price	NTIS Price Code
001-025	\$ 5.00	A02	151-175	\$11.00	A08	301-325	\$17.00	A14	451-475	\$23.00	A20
026-050	6.00	A03	176-200	12.00	A09	326-350	18.00	A15	476-500	24.00	A21
051-075	7.00	A04	201-225	13.00	A10	351-375	19.00	A16	501-525	25.00	A22
076-100	8.00	A05	226-250	14.00	A11	376-400	20.00	A17	526-550	26.00	A23
101-125	9.00	A06	251-275	15.00	A12	401-425	21.00	A18	551-575	27.00	A24
126-150	10.00	A07	276-300	16.00	A13	426-450	22.00	A19	576-600	28.00	A25
									601-up	†	A99

†Add \$1.00 for each additional 25-page increment or portion thereof from 601 pages up.

LASL
REPORT LIBRARY

MAR -5 1961

RECEIVED